

Effect of citric acid on formation of oxides of Cu and Zn in modified sol-gel process: A comparative study

KAMARAJ MAHENDRAPRABHU and PERUMAL ELUMALAI*

Electrochemical Energy and Sensors Lab, Department of Green Energy Technology,
Madanjeet School of Green Energy Technologies, Pondicherry University,
Puducherry 605 014, India
e-mail: drperumalelumalai@gmail.com; elumalai.get@pondiuni.edu.in

MS received 19 December 2015; revised 10 February 2016; accepted 16 March 2016

Abstract. We report here the influence of citric acid concentration on the formation of sol-gel products in each of Cu and Zn systems by using respective metal nitrate as precursor and citric acid as gelling agent. The synthesized sol-gel products were characterized by X-ray diffraction (XRD), scanning electron microscope (SEM), energy dispersive X-ray analysis (EDX), Fourier transform infra-red (FT-IR) spectroscopy and UV-Visible diffused reflectance spectroscopy (UV-Vis DRS). The influence of citric acid concentration on the formation of metal/metal oxide in each case was primarily investigated by varying the molar ratio of each metal nitrate (N) and citric (C) acid (N:C = 1:1, 1:2, 1:4, 1:6 and 1:8). It was observed that at low N:C molar ratios (1:1) and (1:2), the Cu system had only CuO and at high N:C molar ratio, lower oxidation state of copper (Cu₂O and Cu) has resulted. Distinctly, irrespective of the N:C molar ratio, the sol-gel product of Zn system was only single phase of ZnO. The SEM observations confirmed that the grains of these two metal systems were spherical in nature. In each metal system, at high N:C molar ratio, small grain size has resulted. At high N:C ratio, lower oxidation state of metal ion is resulted where the metal system is susceptible for reduction. The susceptibility of metal ions to undergo reduction controlled the formation of end products in the sol-gel process.

Keywords. Sol-gel process; citric acid; copper oxide; zinc oxide; nanocomposite.

1. Introduction

Nanostructured transition-metal oxides (TMOs) have greatly attracted attention for wide range of applications such as sensors, catalysts, lithium-ion batteries, supercapacitors, dye-sensitized solar cells, dielectric devices, luminescence, etc. owing to their fascinating properties with different morphologies (size, shape and distribution).^{1–7} It is well-known that the fascinating properties of the nanostructured materials arises mainly because of enhanced surface-to-volume (S/V) ratio and changes in the density of states (DOS) as a result of spatial confinement.^{8,9} Among the various Transition Metal Oxides (TMO), NiO (nickel oxide), CuO (copper oxide) and ZnO (zinc oxide) are multifunctional materials with numerous applications.^{10–12} Nanostructured CuO finds several applications. For example, Deng *et al.*, reported 3D nano-architected CuO as high-performance supercapacitor material.¹³ Steinhauer *et al.*, utilized CuO nanowires for gas sensing application to detect toxic CO and H₂S.¹⁴ Tian *et al.*, reported nanocomposite comprised of CuO-Cu₂O-Cu nanorods with decorated reduced graphene oxide for photocurrent

generation application.¹⁵ Zoolfakar *et al.*, utilized nanostructured CuO for ethanol vapour sensors.¹⁶ Being a wide band gap semiconductor material ($E_g = 3.37$ eV), ZnO also finds extensive applications in solar cells, optoelectronics, photocatalyst, etc. Wang *et al.*, reported that nanostructured ZnO enhanced the conversion efficiency upto 12% in TiO₂-based dye sensitized solar cells.¹⁷ Muguerra *et al.* fabricated solid-state organic dye-sensitized solar cells using ZnO nanowires as photoelectrodes.¹⁸ Shi *et al.*, examined ZnO nanorods and nanoprisms for NO₂ sensing application.¹⁹ In all these applications, the performance was correlated to the nanosize and composition of the respective oxides.

Several synthetic methods such as hydrothermal, sol-gel, electrochemical deposition, microwave, sonochemical etc. have been adopted for obtaining each of CuO and ZnO-based nanomaterials.^{13–19} Among them, the modified sol-gel process (also known as Pechini method) is regarded as an excellent route because of its simplicity which includes low cost and relatively lower temperatures.^{13–19} The process involves dissolution of metal-ion precursors (for example, metal nitrates) in a suitable solvent and obtaining gel by addition of a gelling agent/chelating agent (citric acid). Usually, a certain ratio of metal nitrate and citric acid

*For correspondence

was used to get respective metal oxides. For example, Dhanasekaran *et al.*, prepared nanostructured CuO using copper nitrate and sodium carbonate as precursors by sol-gel route.²⁰ They have used 0.4 M sodium carbonate and 0.2-0.6 M copper nitrate. Lin *et al.*, investigated variation of band gap of size-controlled ZnO quantum dots by sol-gel process.²¹ Recently, we have reported that the citric acid concentration had a strong influence on the formation of Ni/NiO composition in sol-gel process.²² It was observed that the residual carbon leads to reduction of Ni²⁺ to Ni. To the best of our knowledge, there are no reports on influence of metal nitrate /citric acid (N/C) ratio on the formation of products in sol-gel method for both Cu and Zn systems. So, an attempt has been made to compare the formation of sol-gel end products in these two different metal systems, where one metal ion is susceptible for reduction (Cu²⁺) and other one is non-susceptible for reduction (Zn²⁺). The detailed synthetic process and characterization of sol-gel end products are reported here.

2. Experimental

2.1 Materials and Methods

Each metal oxide or composite was prepared by means of nitrate-citrate based modified sol-gel route. Chemicals such as Cu(NO₃)₂·6H₂O, Zn(NO₃)₂·6H₂O and citric acid (C₆H₈O₇) were of analytical grade (Fisher Scientific, 99%) and used as received. Deionized water was used throughout the experiment. The molar ratio of metal nitrate to citric acid (N:C molar ratio) was varied from 1:1-1:8 (1:1, 1:2, 1:4, 1:6 and 1:8) in each case. Figure 1 shows the schematic view of the sol-gel process adopted in the present work. An appropriate amount of each of metal nitrate was dissolved in deionized water and stirred well for complete dissolution at 80°C for 1 h. To this hot nitrate solution, citric acid solution was added in dropwise and the temperature was increased to 130°C to form sol. The sol was allowed for digestion at 130°C for 6 h to form gel. Then, the gel was dried at the same temperature. Finally, the dried gel was calcined in a furnace at 500°C for 3 h in air to obtain sol-gel product.

The thermogravimetric (TG) and differential thermal analysis (DTA) were done on the gel using thermal analyzer (TA instruments, Q600 SDT and Q20 DSC). The crystal structure and phase identification of as-synthesized sol-gel products were characterized by powder X-ray diffraction (XRD) analysis by using diffractometer (Bruker D8 Advanced) equipped with Cu K_α radiation (wavelength, $\lambda = 1.5418 \text{ \AA}$). Fourier

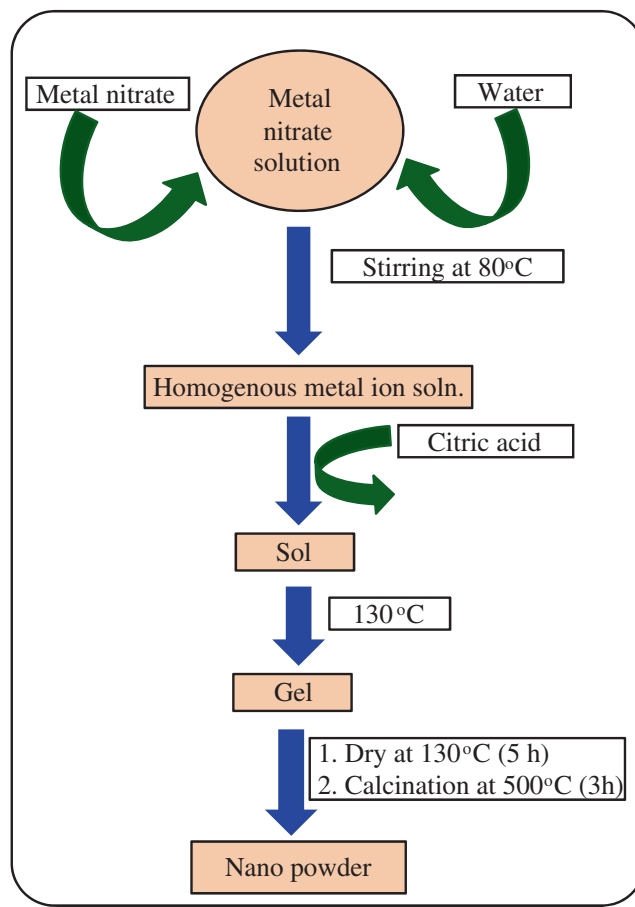


Figure 1. Schematic of the modified sol-gel process adopted in the present work.

transform infra-red spectroscopy data were obtained by using FT-IR spectrometer (Thermo Nicolet 6700) in the frequency range of 500-4000 cm⁻¹. The surface morphology and elemental analysis of the samples were carried out by using scanning-electron microscope equipped with elemental microanalysis system (SEM/EDX - Hitachi S3400N). The UV-Visible diffuse reflectance spectra were recorded by using UV-DR spectroscopy (Varian 5000 UV-vis NIR spectrophotometer) in the wave-length range of 200-1000 nm.

3. Results and Discussion

3.1 Crystal structure of sol-gel end products

To select the calcination temperature, the decomposition of the gel was monitored by TGA/DTA. Figure 2 shows representative data for the gel obtained from (1:8) NC ratio of copper nitrate and citric acid. It can be seen that at 100°C, there is a weight loss which is due to the loss of water molecules from the gel. There is another large weight loss starting at 450°C. This is

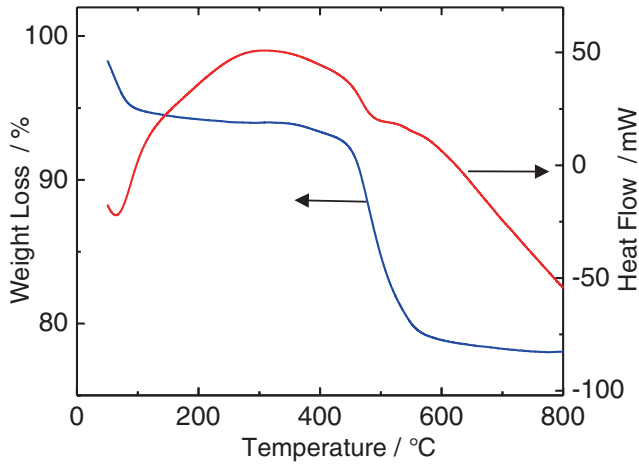


Figure 2. TGA/DTA curves recorded in air for the gel obtained from (1:8) NC ratio of copper nitrate and citric acid.

due to decomposition of the gel. So, the calcination temperature of 500°C was set for both the samples.

The crystal structure and phase identification of the samples were carried out by XRD. Figure 3 shows the XRD patterns of the samples obtained from each of the various N:C molar ratios of Cu system. For the samples obtained from lower N:C molar ratios (1:1 and 1:2), the set of Bragg peaks observed at diffraction angles (2θ), 32.5, 35.5, 38.8, 48.7, 53.8, 58.3 and 61.6° are assigned to the monoclinic phase of CuO as per the standard JCPDS PDF # 895899. For the sample obtained from 1:4 molar ratio, the set of Bragg peaks at diffraction angles (2θ), 32.5, 35.5, 38.8, 48.7, 53.8, 58.3 and 61.6° could be indexed to the monoclinic phase of CuO, while the set of Bragg peaks appeared at 36.4 and 42.3° correspond to the cubic phase of Cu₂O as per the standard XRD pattern of JCPDS # 782076. Interestingly, for the samples obtained from the higher N:C molar ratios (1:6 and 1:8), apart from the peaks for CuO and Cu₂O, the set of high intense Bragg peaks located at 43.3 and 50.44° are assigned to the cubic phase of metallic Cu as per the standard XRD pattern of JCPDS # 892838. Thus, at low N:C ratio, higher oxidation state of copper has resulted (CuO), while at high N:C molar ratio, the sol-gel product resulted in lower oxidation state of copper ion (Cu₂O and metallic Cu). It can be seen that there is gradual reduction of Cu²⁺ (CuO) to Cu⁺ (Cu₂O) and Cu⁺ (Cu₂O) to Cu⁰ as the N:C molar ratio increased, indicating strong influence of citric acid on the formation of sol-gel products.

Figure 4 shows the XRD patterns of the samples obtained from each of the various N:C molar ratios of Zn system. Irrespective of the N:C molar ratio, the observed Bragg peaks were indexed to the hexagonal phase of ZnO as per the standard JCPDS PDF # 800075. Thus, irrespective of N:C molar ratio, single

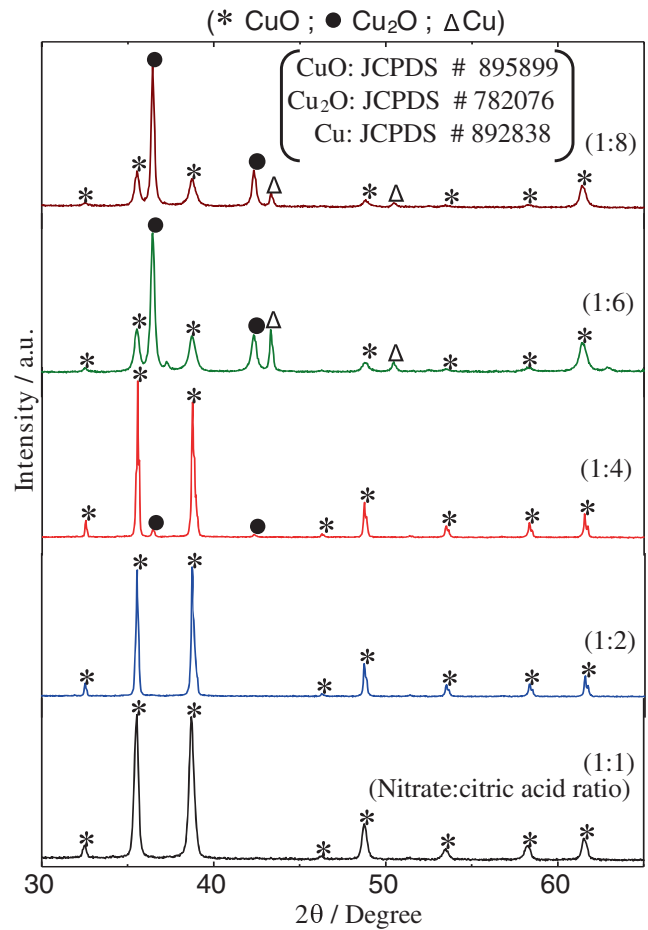


Figure 3. XRD patterns of the samples obtained from each of various N:C molar ratios (1:1-1:8) of copper nitrate and citric acid.

phase of ZnO was resulted, indicating that there is no effect of citric acid on the formation of sol-gel product.

The amount of products formed in both the metal systems have been quantified from the intensity of Bragg peaks. The table 1 shows the obtained data. It is noted that in Cu system, 1:1 and 1:2 N/C ratios resulted in almost 100% of CuO, while at high N/C ratio (1:8), a mixture of CuO (10%), Cu₂O (30%) and Cu (60%) has resulted. It is clear that more amount of lower oxidation state has resulted in Cu system at high N/C ratio. Undoubtedly, for Zn system, in all N/C ratios, only ZnO (100%) was obtained. Thus, the low N/C ratio (1:1) should be used to get pure CuO (Cu²⁺). If mixture of CuO, Cu₂O and Cu is desired, the N/C ratio should be at least 1:6 or above. In the case of Zn system, it is recommended to use any N/C ratio to get ZnO.

Since single phase was obtained in Zn system, the average crystallite size of ZnO was calculated from Bragg peak by using Scherrer formula given below.

$$L_{hkl} = 0.9\lambda / \beta \cos \theta \quad (1)$$

where, L_{hkl} denotes crystallite size, λ is X-ray wavelength (1.5418 Å), β is the full width at half maximum (FWHM) of the Bragg peak (in radians), and θ is the Bragg angle. The obtained ZnO crystallite sizes from 1:1, 1:2, 1:4, 1:6 and 1:8 (N:C) molar ratios are about 70, 64, 56, 41 and 35 nm, respectively.

Figure 5 shows the FT-IR spectra of the sol-gel products obtained from representative N:C molar ratios for both Cu and Zn systems. The strongest peak appeared at about 600 cm^{-1} confirms the presence of metal-oxygen

(M-O) bond (Cu-O: 560 cm^{-1} and Zn-O: 550 cm^{-1}), irrespective of N:C molar ratio in both the systems. The peak observed at about 1000 cm^{-1} is characteristic for C-H bond which could be due to the presence of partially decomposed products of citric acid. It is noted that as the N:C molar ratio increased, the intensity of the peak at 1000 cm^{-1} is also increased. This is due to presence of more amounts of partially decomposed products of citric acid in both the systems. The broad peak

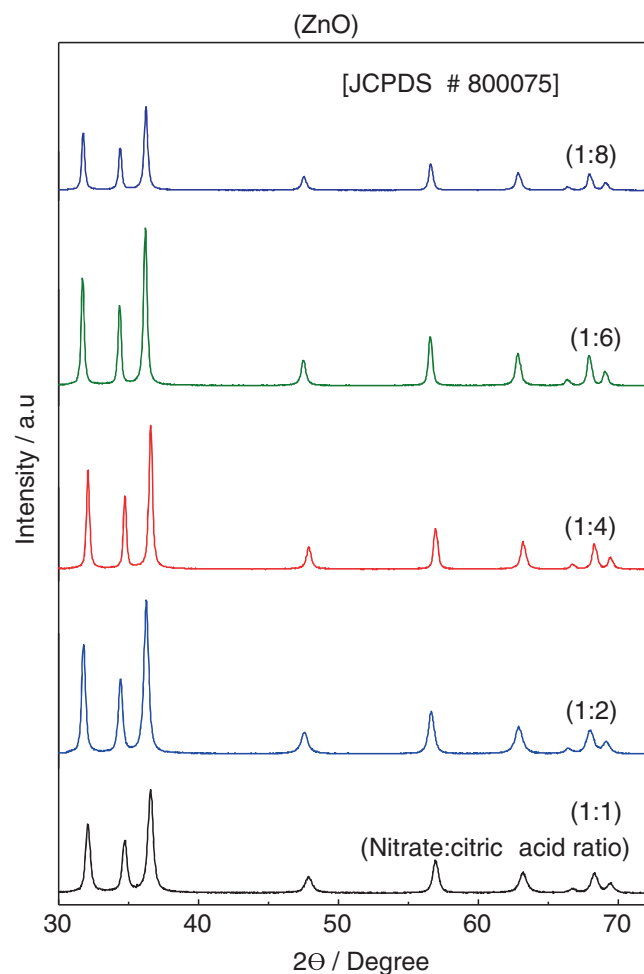


Figure 4. XRD patterns of the samples obtained from each of various N:C molar ratios (1:1-1:8) of zinc nitrate and citric acid.

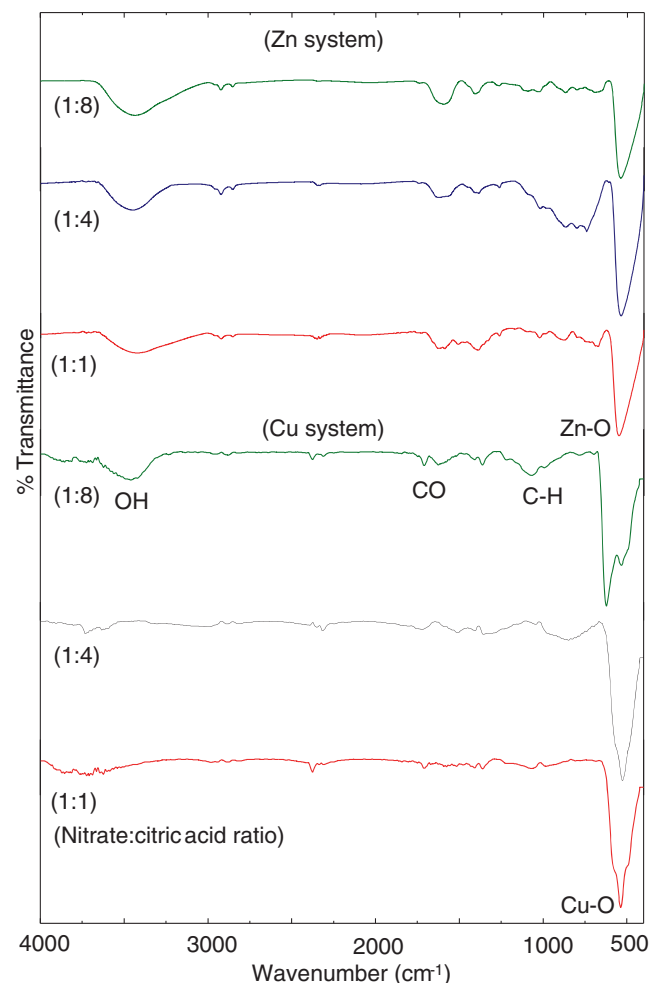


Figure 5. FT-IR spectra of the samples obtained from representative N:C molar ratios (1:1, 1:4 and 1:8) of metal nitrates and citric acid synthesized by modified sol-gel process.

Table 1. The products formed and their amounts (in brackets) in the modified sol-gel process using various N:C molar ratios for Cu and Zn systems.

Metal system	1:1 (Molar ratio)	1:2	1:4	1:6	1:8
Cu	CuO (100%)	CuO (100%)	CuO (90%) Cu ₂ O (10%)	CuO (70%) Cu ₂ O (20%) Cu (10%)	CuO (10%) Cu ₂ O (30%) Cu (60%)
Zn	ZnO (100%)	ZnO (100%)	ZnO (100%)	ZnO (100%)	ZnO (100%)

appeared at about 3600 cm^{-1} is ascribed to OH group of adsorbed water molecules which could have come either from decomposition of citric acid or atmosphere. The peak observed at about 1600 cm^{-1} is characteristic for CO which could be due to the presence of partially decomposed products of citric acid. The amount of partially decomposed products in the forms of CO and CH are more at high N:C molar ratios. Thus, the IR spectra confirm that, in each case, along with the respective oxides partially decomposed products of citric acid is present in the sol-gel product. It should be noted that the calcination temperature was only 500°C which is relatively lower. Thus, CO and CH are present in the samples.

The UV-Visible diffused reflectance studies were done to estimate the optical band gap of ZnO semiconductor. Figure 6 shows the UV-Visible spectra of ZnO samples obtained from 1:1, 1:4 and 1:8 N:C molar ratios. The estimated band gaps of ZnO obtained from 1:1, 1:4 and 1:8 (N:C) molar ratios were 3.39, 3.43 and 3.44 eV, respectively. As the N/C ratio increased, the band gap also increased marginally. This increase in band gap is due to quantum confinement effect associated with the ZnO nano grains. The amount of zinc nitrate / citric acid could be manipulated to achieve still smaller grains having strong quantum confinement. The amount of zinc nitrate could be manipulated to achieve still smaller grain size associated with strong quantum confinement associated with the ZnO nano grain.

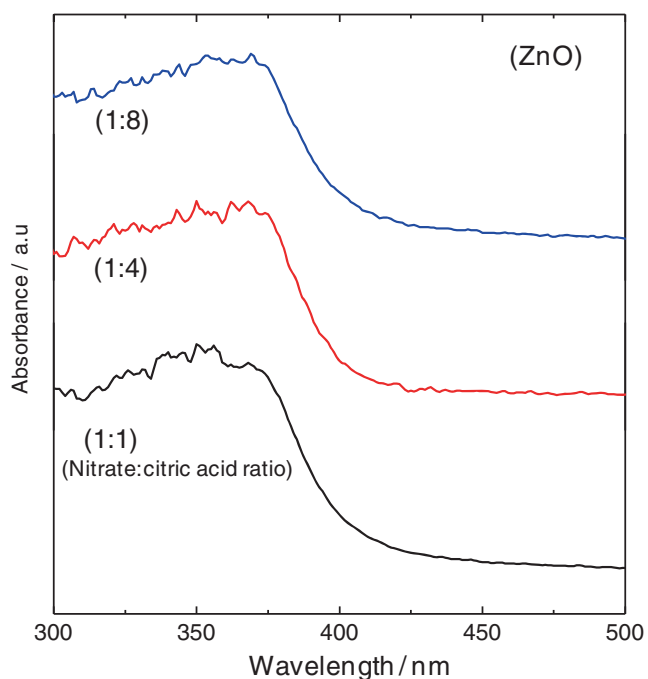


Figure 6. UV-Vis spectra of the samples obtained from representative N:C molar ratios (1:1, 1:4 and 1:8) of zinc nitrate and citric acid synthesized by modified sol-gel route.

3.2 Surface morphology

The surface morphology of the samples (both metal systems) obtained from representative 1:1, 1:4 and 1:8 N:C molar ratios was analyzed by using SEM and the obtained micrographs are shown in figure 7 (a – f). SEM images confirm the formation of almost uniform spherical grains in both the metal systems. At low (N:C) molar ratio, the average grain sizes for Cu and Zn Systems are about 80 and 70 nm, respectively. At high N:C molar ratio (1:8), the average grain sizes for Cu and Zn systems are about 42 and 35 nm, respectively. At 1:4 N/C ratio, a moderate grain size was obtained for both the metal systems. It can be seen that the samples obtained from 1:1 N:C molar ratio had bigger grain size, while the samples obtained from 1:8 molar ratio had smaller grain size. This is because, at high N:C molar ratio, the lower metal content leads to the formation of smaller size grains.

The elemental analysis carried out by EDX (not shown) confirmed the presence of Cu and Zn as the only metallic elements in each matrix. No other impurities were present. Based on the above mentioned XRD, FT-IR and SEM/EDX results, it is clear that the N:C molar ratio played a vital role on the formation of end products in sol-gel process using metal nitrate as precursor and citric acid as gelling agent.

3.3 Explanation for the formation of sol-gel end products

From the XRD and FT-IR data discussed above, in the case of Zn system which is non-susceptible for reduction, irrespective of the N:C molar ratio, only single ZnO phase was obtained. This confirms that though the residual carbon is present in the matrix, zinc ion is unable to undergo reduction to its lower oxidation state or metallic zinc in the present condition. The following reduction reaction is expected in presence of residual carbon at 500°C .



It should be noted that Zn^{2+} ion is not susceptible for reduction because the free energy change of the above reaction (2) (+80 kJ/mol) is not thermodynamically favorable.²³ Because of the highly positive free energy change for the above reaction, the reduction of Zn^{2+} has not occurred even at high N:C molar ratio and 500°C , and zinc remained as Zn^{2+} (as ZnO). This is in accordance with the Ellingham diagram in which the ZnO formation curve is at the bottom (*i.e.*, formation of ZnO is highly feasible).²⁴ On the other hand, in the case of Cu system which is susceptible for reduction, it

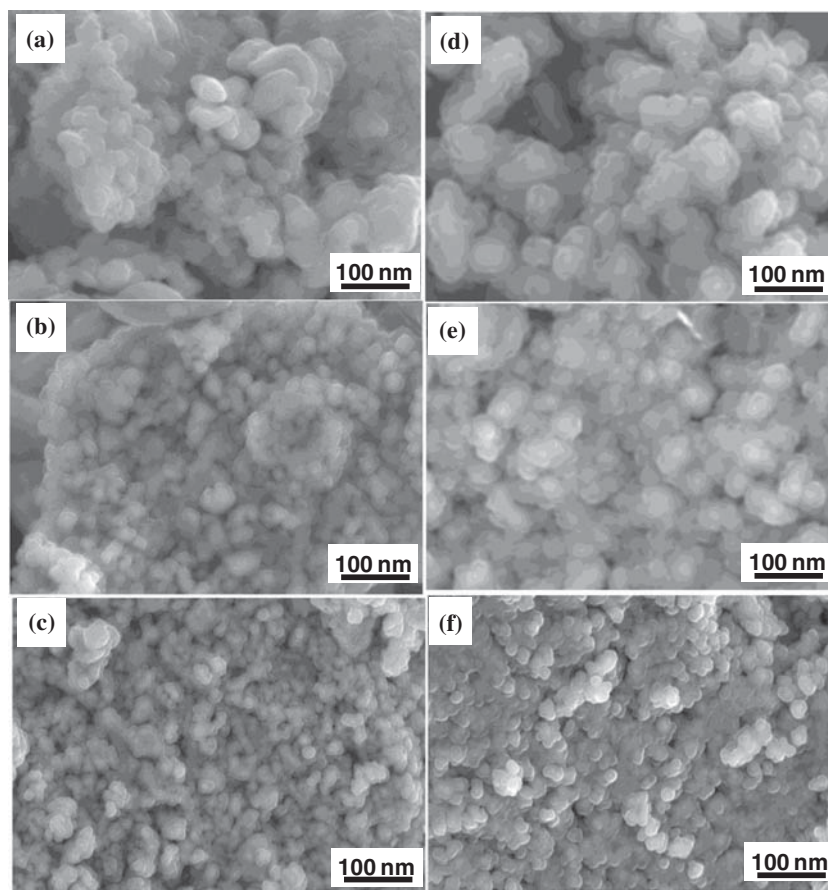
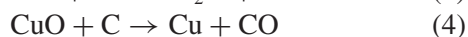
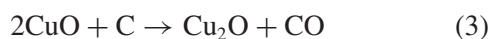


Figure 7. SEM images of surface of the samples from representative N/C ratios (a) (1:1), (b) (1:4) and (c) (1:8) of Cu system, and (d) (1:1), (e) (1:8) and (f) (1:8) of Zn system.

is evidently seen that the concentration of citric acid had strong influence on the formation of sol-gel end product. That is, gradual reduction of Cu^{2+} ion to Cu^+ and even copper metal (Cu^0), as the citric acid concentration is increased. At low citric acid concentration (1:1), amount of residual carbon present is less and no reduction of copper ion occurred. The increased citric acid concentration led to the formation of more residual carbon which reduced significant amount of CuO (Cu^{2+}) to Cu_2O (Cu^+). At high N:C molar ratio (1:8), more amount of Cu_2O and metallic Cu was formed because of high residual carbon content. This confirms that the residual carbon led to reduction of Cu^{2+} (CuO) to Cu^+ (Cu_2O) or even Cu^0 . It is noted that copper ion is susceptible for reduction to lower oxidation state (free energy change: -206 kJ/mol) or even to metal (free energy change: -97 kJ/mol),²³ according to the following reduction reactions.



Thus, the results obey Ellingham diagram for both feasibility for formation of oxides ($\text{ZnO} > \text{CuO}$)

and susceptibility for reduction ($\text{Cu}^{2+} < \text{Zn}^{2+}$).²⁴ It is known that metal nanoparticles are prone to surface oxidation due its high reactivity. However, in this case, the carbon present in the high NC mole ratio samples may stabilize the Cu nanoparticles formed from the reduction of CuO and Cu_2O . Work is under progress using each of these products as electrodes for Li-ion battery and electrochemical gas sensing applications.

4. Conclusions

It was demonstrated that concentration of citric acid had strong influence on the formation of the end products in Cu and Zn systems in the modified sol-gel process. The end products of the sol-gel process are controlled by the susceptibility of metal ions to undergo reduction. The metal ion which is susceptible for reduction (Cu^{2+}), underwent reduction to its lower oxidation (Cu^+) or even to its metallic state (Cu^0), while the metal ion (Zn^{2+}) which is non-susceptible for reduction, did not undergo reduction at all. Thus, proper amount of citric acid concentration should be selected to get

metal/metal oxide nanocomposite or pure nanostructured metal oxide network depending on the nature of metal ions.

Acknowledgements

Authors thank the Department of Science and Technology (DST), Govt. of India, New Delhi, for the financial support (DST/FT/CS-64/2010). CSIR-CECRI at Karaikudi and Chennai and Central Instrumentation Facility - Pondicherry University, Puducherry are acknowledged for characterization supports.

References

- Poizot P, Laruelle S, Grugeon S, Dupont L and Tarascon J M 2000 *Nature* **407** 496
- Deng W, Ji X, Chen Q and Banks C E 2011 *RSC Adv.* **1** 1171
- Zhang Q, Uchaker E, Candelariuz S L and Cao G 2013 *Chem. Soc. Rev.* **42** 3127
- Schelter M, Zosel J, Oelßner W, Guth U and Mertig M 2013 *Sens. Actuators, B* **187** 209
- Yin Y and Talapin D 2013 *Chem. Soc. Rev.* **42** 2484
- Meher S K and Rao G R 2014 *J. Chem. Sci.* **126** 361
- Fujio Y, Xu C N, Terasaki N and Ueno N 2014 *J. Lumin.* **148** 89
- Yu M, Long Y Z, Sun B and Fan Z 2012 *Nanoscale* **4** 2783
- Goriparti S, Miele E, Angelis F D, Fabrizio E D, Zaccaria R P and Capiglia C 2014 *J. Power Sources* **257** 421
- Kim H J and Lee J H 2014 *Sens. Actuators, B* **192** 607
- Chen X, Li C, Gratzel M, Kostecki R and Mao S S 2012 *Chem. Soc. Rev.* **41** 7909
- Rai A K, Anh L T, Park C J and Kim J 2013 *Ceram. Int.* **39** 6611
- Deng M J, Wang C C, Ho P J, Lin C M, Chen J M and Lu K T 2014 *J. Mater. Chem. A* **2** 12857
- Steinhauer S, Brunet E, Maier T, Mutinati G C, Köck A, Freudenberg O, Gspan C, Grogger W, Neuhold A and Resel R 2013 *Sens. Actuators, B* **87** 50
- Tian J, Li H, Xing Z, Wang L, Luo Y, Asiri A M, Youbi A O A and Sun X 2012 *Catal. Sci. Technol.* **2** 2227
- Zoolfakar A S, Ahmad M Z, Rani R A, Ou J Z, Balendhran S, Zhuiykov S, Latham K, Wlodarskia W and Zadeh K K 2013 *Sens. Actuators, B* **185** 620
- Wang G, Cai Z, Li F, Tan S, Xie S and Li J 2014 *J. Alloys. Compd.* **583** 414
- Muguerra H, Berthoux G, Yahya W Z N, Kervella Y, Ivanova V, Boucle J and Demadrille R 2014 *Phys. Chem. Chem. Phys.* **16** 7472
- Shi L, Naik A J T, Goodall J B M, Tighe C, Gruar R, Binions R, Parkin I and Dar J 2013 *Langmuir* **29** 10603
- Dhanasekaran V, Soundaram N, Kim S I, Chandramohan R, Mantha S, Saravanakumar S and Mahalingam T 2014 *New J. Chem.* **38** 2327
- Lin K F, Cheng H M, Hsu H C, Lin L J and Hsieh W F 2005 *Chem. Phys. Lett.* **409** 208
- Mahendraprabhu K and Elumalai P 2015 *J. Sol-Gel Sci. Technol.* **73** 428
- Robie R A, Hemingway B S and Fisher J R 1979 *U.S. Geological Survey Bulletin* **1452** 241
- Ellingham H J T 1944 *J. Soc. Chem. Ind. (London)* **63** 125